Matrix Isolation Study of FeCr Molecules and SCF-Xα-Scattered Wave Molecular Orbital Calculations on Fe_2 and FeCr Diatomics

H. M. Nagarathna,[†] Pedro A. Montano,*[†] and Vaman M. Naik[‡]

Contribution from the Department of Physics, West Virginia University, Morgantown, West Virginia 26506, and the Biophysics Research Division, University of Michigan, Ann Arbor, Michigan 48109. *Received June 11, 1982*

Abstract: Rare gas matrix isolation techniques have been used in conjunction with Mössbauer spectroscopy to study the bimetallic molecules of iron and chromium. Various molecules were identified by concentration dependence studies and Monte Carlo calculations. Temperature dependence studies were also carried out with a closed-cycle helium refrigerator. Fe_2 molecules trapped in Kr matrices at (15–40 K) showed quadrupole splitting (QS) of 3.78 ± 0.06 mm/s and an isomer shift (IS) = 0.06 ± 0.06 mm/s which are slightly different from the Mössbauer parameters of Fe_2 molecules in Ar or Kr matrices at 4.2 K. These experiments also indicated an enhanced diffusion of Cr atoms in argon matrices at (15–40 K) forming larger bimetallic clusters even at very low concentrations. SCF-Xα-scattered wave (SW) calculations were employed to study the nature of electronic bonding between Fe–Fe and Fe–Cr atoms in Fe_2 and FeCr diatomic molecules. The most probable electronic ground state for Fe_2 is $^7\Sigma_g$ ($\sigma_g^2\pi_u^4\sigma_g^2\delta_g^2\delta^*{}_u^2\pi^*{}_g^2\sigma^*{}_u^2$) consistent with the measured sign and magnitude of QS as well as the measured equilibrium internuclear distance. For FeCr molecules either $^7\Sigma$ or $^7\Delta$ is the probable electronic ground state indicating a ferromagnetic coupling between Fe and Cr atoms.

Introduction

The study of small metallic and bimetallic clusters is of great interest in areas such as surface physics and chemistry, nucleation, heterogeneous catalysis, and alloy formation.[1] Metal clusters represent a situation intermediate between the free atom and bulk metal. A number of theoretical treatments of chemisorption and surface reactions have used the model of a small cluster based on the assumption that relatively small metal clusters exhibit bulk properties.[1] Numerous sophisticated techniques both theoretical and experimental have been applied to investigate these systems. Molecular orbital methods such as Extended Hückel,[2] SCF-Xα,[3] and ab initio methods[4] have been used to investigate the electronic structures as a function of size and geometry of these clusters, and valuable information has been obtained. Rare gas matrix isolation techniques have been used in conjunction with Mössbauer spectroscopy, optical absorption spectroscopy, and ESR to study the electronic structure of the diatomic molecules such as Fe_2,[5,6] FeCo,[7] FeMn,[8] FeNi,[9] FeCu,[10] Cr_2, Mo_2, CrMo,[11] CuMg, AuMg,[12] and higher aggregates.[13] Just as homonuclear diatomic molecules provide a useful reference point for theoretical studies of the chemisorption and catalytic properties of larger aggregates, the heteronuclear diatomics will prove to be equally valuable for theoretical modelling of alloying clusters as a function of size and geometry.[11]

In this study, we have extended the rare gas matrix isolation studies of transition metal clusters to include iron–chromium clusters. SCF-Xα-SW[14] molecular orbital technique is employed to probe the electronic and bonding properties of Fe_2 and FeCr diatomic molecules.

Experimental Procedures

The experiments were performed at 4.2 K with a liquid helium cryostat and at higher temperatures (15–40 K) with a closed cycle He refrigerator. The sample chamber was evacuated to a pressure less than 10^{-7} torr. Atomic beams of iron (90% enriched ^{57}Fe) and Cr were produced in two alumina crucibles contained in a resistance-heated tantalum furnace. The metal deposition rates were calculated using previously measured collection efficiencies. The atomic beams were codeposited with a rare gas (Ar or Kr) onto an Al disk (ultrahigh purity) maintained at low temperature by thermal contact with the bath. The rare gas deposition rate was continuously monitored by the attenuation of 6.3 keV X-ray or 14.4 keV γ-ray of a ^{57}Co–Rh source. The isomer shifts (IS) are given with respect to α-iron at room temperature. The species were identified by concentration dependence studies and Monte Carlo calculations.[7] The samples prepared with the closed-cycle He refrigerator (15–40 K) showed the formation of much larger aggregates and in greater abundance than those predicted by a simple random model. There was also an indication of enhanced diffusion of Cr atoms in argon matrices as compared to Fe. The gas composition and residual gases in the system were analyzed with a mass spectrometer, partial pressure of O_2 being less than 10^{-9} torr during deposition as compared to 4×10^{-5} torr for argon or krypton.

Experimental Results and Discussion

The Mössbauer spectrum at 4.2 K of a sample of 0.08 at. % metal in argon (Fe/Cr = 3:1) is shown in Figure 1. From probability considerations one would expect to see only monomers at this concentration, but because of the migration of the species at the sample surface during deposition, multimers are also observed.[7-9] The best fit to the spectrum was obtained with a singlet and 4 quadrupole doublets. The singlet had an IS = −0.75 ± 0.06 mm/s and was identified as due to iron monomers (Fe_0).[5,7] The doublet with an IS = −0.12 ± 0.06 mm/s and a quadrupole splitting (QS) = 4.08 ± 0.06 mm/s was identified as that of iron dimers Fe_2.[5,7-9] The doublet with an IS = 0.12 ± 0.05 mm/s and a QS = 2.94 ± 0.05 mm/s with a line width of 0.85 ± 0.15 mm/s was tentatively assigned to FeCr dimers. The assignment was further confirmed from experiments at other metal concentrations. Also, the IS and QS values of FeCr molecules match well with those of the previously identified molecules such as FeMn, FeCo,

[†] West Virginia University.

[‡] University of Michigan.

(1) G. A. Ozin, *Catal. Rev. Sci. Eng.*, **16**, 191 (1977).
(2) R. C. Baetzold, *Adv. Catal.*, **25** (1976).
(3) C. Y. Yang, K. H. Johnson, D. R. Salahub, J. Kaspar, and R. P. Messmer, *Phys. Rev. B*, **24**, 5673 (1981).
(4) J. Demuynck, M. Rohmer, A. Strich, and A. Veillard, *J. Chem. Phys.*, **75**(7), 3443 (1981); C. Wood, M. Doran, I. M. Hillier, and M. F. Guest, *Symp. Faraday Soc.*, **14**, 159 (1980).
(5) P. H. Barrett and T. K. McNab, *Phys. Rev. Lett.*, **25**, 1601 (1970); T. K. McNab, H. Micklitz, and P. H. Barrett, *Phys. Rev. B*, **4**, 3787 (1971); T. C. Devore, A. Ewing, H. F. Franzen, and V. Calder, *Chem. Phys. Lett.*, **35**, 78 (1975).
(6) M. Moskovits and D. P. DiLella, *J. Chem. Phys.*, **73**(10), 4817 (1980); C. Cosse, M. Fonassier, T. Mejean, M. Tranquille, D. P. DiLella, and M. Moskovits, *J. Chem. Phys.*, **73**, 6076 (1980).
(7) W. Dyson and P. A. Montano, *Phys. Rev. B*, **20**, 3619 (1979).
(8) W. Dyson and P. A. Montano, *J. Am. Chem. Soc.*, **100**, 7439 (1978); *Solid State Commun.*, **33**, 191 (1980).
(9) P. A. Montano, *J. Appl. Phys.*, **49**, 1961 (1978); P. A. Montano, *Symp. Faraday Soc.*, **14**, 79 (1980).
(10) P. A. Montano and M. A. Talarico, *J. App. Phys.*, **50**, 2405 (1979).
(11) W. Klotzbücher, G. A. Ozin, J. G. Norman, Jr., and H. J. Kolari, *Inorg. Chem.*, **16**, 2871 (1977).
(12) P. H. Kasai and D. Mcleod, Jr., *Symp. Faraday Soc.*, **14**, 65 (1980).
(13) H. M. Nagarathna, H. J. Choi, and P. A. Montano, *Trans. Faraday Soc.*, **78**, 923 (1982).
(14) J. C. Slater and K. H. Johnson, *Phys. Rev.*, *B*, **5**, 844 (1972).

0002-7863/83/1505-2938$01.50/0

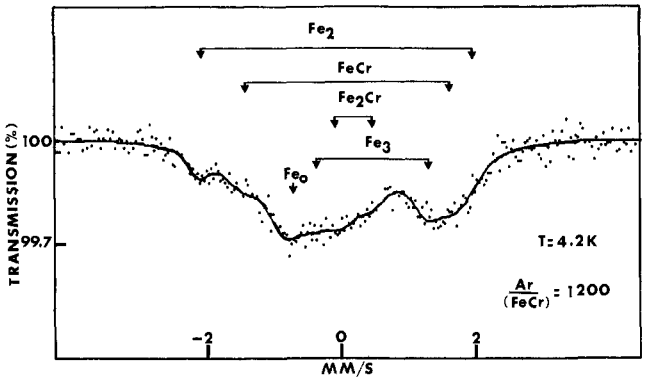

Figure 1. Mössbauer spectrum of (FeCr)–Ar at 4.2 K, 0.08 at. % metal concentration (continuous curve is the fit to the experimental data).

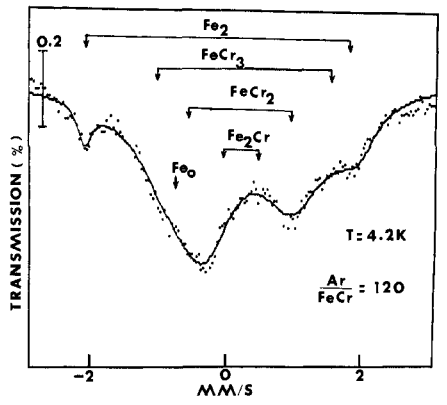

Figure 2. Mössbauer spectrum of (FeCr)–Ar at 4.2 K, 0.83 at. % metal concentration.

Fe_2, FeNi, etc.[7-9] Since Fe/Cr = 3:1, the probability of the formation of Fe_2Cr and Fe_3 species is larger than $FeCr_2$. Hence, the doublet with IS = 0.42 ± 0.05 mm/s and QS = 1.65 ± 0.05 mm/s was assigned to Fe_3 molecules in agreement with reported measurements.[7] The remaining doublet with IS = 0.2 ± 0.1 mm/s and QS = 0.44 ± 0.10 mm/s was assigned to Fe_2Cr molecules.

In order to study the concentration dependence of the iron–chromium molecules, we carried out measurements at higher metal to argon ratio (argon/metal = 120) (Figure 2). In this case Fe/Cr = 1:2 and consequently the trimeric and higher multimers of iron–chromium are possible. The identified species are Fe_0, Fe_2, Fe_2Cr, and some Fe_3 (and possibly Fe_4). The dominant doublet with an IS = 0.25 ± 0.10 mm/s and QS = 1.26 ± 0.10 mm/s is assigned to $FeCr_2$ molecules because the matrix is Cr rich. There was an indication of a small amount of FeCr molecules. The appearance of another doublet with IS = 0.3 ± 0.10 mm/s and QS = 2.74 ± 0.10 mm/s might be due to $FeCr_3$ or Fe_2Cr_2 molecules. The absence of a large number of FeCr molecules and the presence of Cr-rich multimers may be due not only to a higher concentration of Cr but also to the enhanced diffusion of Cr in argon matrices observed during a large number of test runs.

Samples prepared with the closed cycle He refrigerator (15–40 K) reveal quite different Mössbauer spectra. Figure 3 shows the spectra of iron–chromium molecules in krypton at various temperatures. The doublet having a line width of 0.40 ± 0.06 mm/s and with IS = 0.06 ± 0.06 mm/s and QS = 3.78 ± 0.06 mm/s is evident in the spectra. The same doublet was present when a completely different system (Fe–Pt/Kr) was studied. Similar doublets in different samples indicated that they are due to the same species. The large QS and narrow line width suggest that the doublet is essentially due to Fe_2 molecules in Kr at higher temperatures. The different values for the Mössbauer parameters of the Fe_2 molecules in Kr matrices at 15–40 K are probably due to the population of electronic excited states of Fe_2, resulting in a reduction in the electric field gradient (EFG) at the ^{57}Fe nucleus as compared to the value at 4.2 K. The FeCr molecules showed

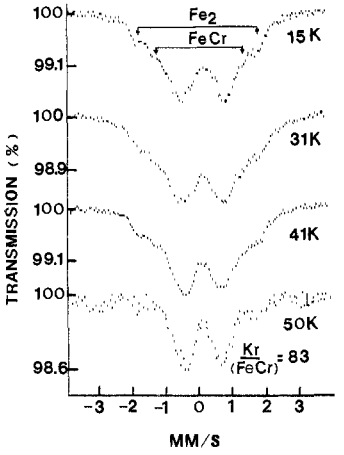

Figure 3. Mössbauer spectra of (FeCr)–Kr at 15–50 K, 1.2 at. % metal concentration.

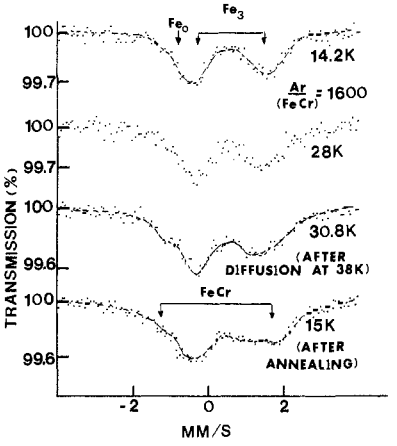

Figure 4. Mössbauer spectra of (FeCr)–Ar at 14–31 K, 0.06 at. % metal concentration.

Table I. Metal Clusters Observed and Their Mössbauer Parameters

species	matrix	T, K	IS, mm/s	QS, mm/s	line width, 2Γ, mm/s
Fe^0	Ar	4.2	−0.75 ± 0.06		1.2 ± 0.1
Fe_2	Ar	4.2	−0.12 ± 0.06	4.08 ± 0.06	0.47 ± 0.06
Fe_2	Kr	15	0.06 ± 0.06	3.78 ± 0.06	0.40 ± 0.06
Fe_3	Ar	4.2	0.42 ± 0.10	1.65 ± 0.10	1.00 ± 0.10
Fe_3	Ar or Kr	15	0.55 ± 0.06	1.65 ± 0.10	1.00 ± 0.10
FeCr	Ar	4.2	0.12 ± 0.05	2.94 ± 0.05	0.85 ± 0.10
FeCr	Ar	15	0.15 ± 0.10	3.10 ± 0.10	0.90 ± 0.10
FeCr	Kr	15	0.17 ± 0.06	2.90 ± 0.06	0.85 ± 0.06
Fe_2Cr	Ar	4.2 or 15	0.20 ± 0.10	0.44 ± 0.10	1.00 ± 0.10
$FeCr_2$	Ar or Kr	4.2 or 15	0.25 ± 0.10	1.26 ± 0.10	1.00 ± 0.10
$FeCr_3$, Fe_2Cr_2	Ar	4.2	0.30 ± 0.10	2.74 ± 0.10	1.0 ± 0.10
Fe_nCr_m[a]	Ar	4.2	0.40 ± 0.15	0.2 ± 0.15	
Fe_nCr_m[b]	Ar	15	0.5 ± 0.15		

[a] $n = 2, 3; m \geq 3$. [b] $n \geq 2; m \geq 2$.

IS = 0.17 ± 0.06 and QS = 2.90 ± 0.06 mm/s, which is within the experimental error the same value obtained in Ar at 4.2 K. The central doublet is due to the trimeric species. At 50 K, the spectrum indicated the formation of larger clusters. This is attributed to the high mobility of the atoms in krypton at higher temperatures.

The samples prepared in the closed cycle He refrigerator using an argon matrix showed a high degree of diffusion forming larger aggregates even at very low metal concentration. Particularly Cr shows an enhanced diffusion in the argon matrices which is evident

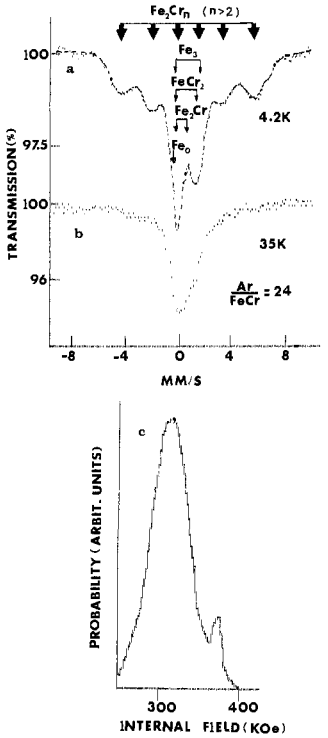

Figure 5. (a) Mössbauer spectrum of (FeCr)–Ar at 4.2 K, 4.0 at. % metal concentration; (b) Mössbauer spectrum at 35 K; (c) magnetic hyperfine fields distribution at the ^{57}Fe nucleus for this sample.

from Figure 4. These spectra were obtained with a sample with 0.06 at. % metal in argon with Fe/Cr = 7:1 at various temperatures. The species present are indicated in the spectra. As the temperature is increased, the concentrations of FeCr and trimeric species ($FeCr_2$, Fe_2Cr) are enhanced (Mössbauer parameters listed in Table I). This is related to the strong mobility of Cr in the matrix.

Very high metal concentration samples showed magnetic hyperfine splitting at 4.2 K. The spectrum of a sample with argon/metal = 22 and Fe/Cr = 1:7 is shown in Figure 5a. The best fit was obtained with three sets of magnetically split peaks in addition to Fe_0 and trimeric species. The large line widths may be due to clusters of various sizes and different ^{57}Fe sites in a given cluster. The distribution of magnetic hyperfine fields is shown in Figure 5c. The average hyperfine field was around 310 kOe with IS = 0.40 ± 0.15 mm/s and QS = 0.20 ± 0.15 mm/s. According to Monte Carlo calculations, the expected species higher than trimers are $FeCr_3$ and $FeCr_4$, but due to the diffusion of the atoms, we might expect species such as Fe_nCr_m with $n = 2, 3$ and $m \geq 3$. The observation of a positive IS for the iron chromium clusters is in striking contrast with FeCr alloys (where IS is slightly negative).[15] In none of the FeCr alloys is such a positive IS observed. This result is very similar to that of FeMn clusters compared to FeMn alloys.[8] In this sense, the small clusters of FeCr may not represent bulk alloys. When the matrix was heated to 35 K, there was a collapse of the hyperfine field as shown in Figure 5b. This might be due either to spin relaxation effects or to Cr diffusion resulting in a large number of Cr atoms surrounding the ^{57}Fe atom giving no hyperfine splitting at the ^{57}Fe nucleus.[15]

The spectrum of a high metal concentration (argon/metal = 42, Cr/Fe = 2:1) sample prepared with the closed-cycle helium refrigerator differed markedly from the spectrum at 4.2 K. It revealed a magnetic hyperfine split spectrum with an average hyperfine field of 110 kOe and IS = 0.50 ± 0.15 mm/s. The smaller splitting may be due to spin relaxation effects or to Cr

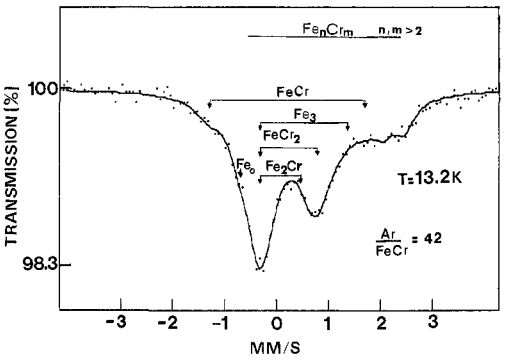

Figure 6. Mössbauer spectrum of (FeCr)–Ar at 13 K, 2.4 at. % metal concentration.

atoms surrounding the ^{57}Fe atom and decreasing the magnetic moment at the ^{57}Fe atom (Figure 6). Table I lists the Mössbauer parameters of all the species identified.

SCF–Xα–SW Calculations for Fe_2 and FeCr Molecules

Recently one-electron properties of small molecules have been calculated from Xα–multiple scattered wave functions using muffin tin[14] as well as overlapping spheres approximations[16] with the charge partitioning method.[17] The charge partitioning procedure reproduces one electron properties to the accuracy of the Xα wave function itself.[17] Though the total energy calculated by the present version of the method is not accurate enough to calculate the potential energy surfaces, the one-electron orbitals are calculated accurately[18a] and hence the one-electron properties are accurate enough to compare with the experimental values.

The Xα–SW method has been used in calculating one-electron energy levels of transition metal diatomics such as Cr_2,[11] Mo_2,[11] CrMo,[11] and Ni.[18b] The method has proven useful in cases such as Cr_2, Mo_2, and CrMo to explain the electron absorption spectra using the transition state method.[11]

We have carried out SCF–Xα–SW calculations on Fe_2 and FeCr molecules hoping to find more information about their electronic ground states and hence to probe into the nature of electron bonding between the two transition metal atoms. The Xα–SW functions are used to calculate the one-electron properties such as charge density at the nucleus, electric field gradient, spin density at the nucleus, hyperfine coupling constants, etc., which are used to calculate the Mössbauer parameters such as IS, QS, and magnetic hyperfine field at the nucleus. Mössbauer parameters for Fe_2 molecules are measured very accurately. Fe_2 molecules exhibit a quadrupole doublet with IS = −0.12 ± 0.06 mm/s and QS = 4.08 ± 0.06 mm/s. Montano et al.[19] have measured the hyperfine field at the ^{57}Fe nucleus to be |660 ± 15| kOe and have shown that V_{zz} is negative. FeCr molecules also show a quadrupole doublet with QS = 2.94 ± 0.08 mm/s and IS = 0.12 ± 0.08 mm/s. The sign of V_{zz} could not be determined. It is noted that the Mössbauer lines are broad.

Harris and Jones[20] reported first principle calculations on Fe_2 using the density functional method. They predicted $^7\Delta_u$-$(\sigma_g^2\pi_u^4\sigma_g^2\delta_g^3\delta^{*}_u{}^2\pi^{*}_g{}^2\sigma^{*}_u{}^1)$ as the electronic ground state for Fe_2 with equilibrium distance of 2.1 Å.

Shim and Gingerich[21] carried out ab initio HF–CI calculations of the electronic structure of Fe_2 molecules and predicted $^7\Delta_u$ state with the $(3d\sigma_g)^{1.57}(3d\pi_u)^{3.06}(3d\delta_g)^{2.53}(3d\delta_u{}^{*})^{2.47}(3d\pi_g{}^{*})^{2.89}$-

(15) B. D. Sawicka, J. Sawicki, and J. Stanek, *Phys. Lett.*, **59A**, 59 (1976); L. H. Schwartz and D. Chandra, *Phys. Status Solidi B*, **45**, 201 (1971); G. K. Wertheim, *J. Appl. Phys.*, **32**, 1105 (1961); C. E. Johnson, M. S. Ridout, and T. C. Cranshaw, *Proc. Phys. Soc.*, **81**, 1079 (1963).

(16) F. Herman, A. R. Williams, K. H. Johnson, *J. Chem. Phys.*, **61**, 3508 (1974); J. G. Norman, Jr., *J. Chem. Phys.*, **61**, 4630 (1974).

(17) M. Cook and M. Karplus, *J. Chem. Phys.*, **72**, 7 (1980); D. A. Case, M. Cook, and M. Karplus, *J. Chem. Phys.*, **73**(7), 3294 (1980).

(18) (a) G. A. Ozin, H. Huber, D. McIntosh, S. Mitchell, J. G. Norman, Jr., and L. Noodleman, *J. Am. Chem. Soc.*, **101**, 3504 (1979); J. G. Norman, H. J. Kolari, H. B. Gray, and W. C. Trogler, *Inorg. Chem.*, **16**, 987 (1979); (b) N. Rösch and T. N. Rhodin, *Phys. Rev. Lett.*, **21**, 1189 (1974).

(19) P. A. Montano, P. H. Barrett, and Z. Shanfield, *J. Chem. Phys.*, **64**, 2896 (1976).

(20) J. Harris and R. O. Jones, *J. Chem. Phys.*, **70**, 830 (1979).

(21) I. Shim and K. A. Gingerich, to be published.

Table II. Hyperfine Parameters for Fe_2 (Fe–Fe Distance = 2 Å) (QS without Sternheimer Correction)

	% overlap					
	0		25		30	
configuration	QS, mm/s	mhf,[a] kOe	QS, mm/s	mhf, kOe	QS, mm/s	mhf, kOe
1. $\sigma_g^2\pi_u^4\sigma_g^2\delta_g^3\delta_u^{*2}\pi_g^{*2}\sigma_u^{*1}$ ($^7\Delta_u$)	−2.78	≈0	−2.95	60	−2.78	109
2. $\sigma_g^2\pi_u^4\sigma_g^2\delta_g^2\delta_u^{*2}\pi_g^{*2}\sigma_u^{*1}\sigma_u^{*1}$ ($^9\Sigma_g$)	−6.67	593	−6.84	812	−6.70	858
3. $\sigma_g^2\pi_u^4\sigma_g^2\delta_g^2\delta_u^{*2}\pi_g^{*2}\sigma_u^{*2}$ ($^7\Sigma_g$)	−6.82	−337	−7.14	−350	−7.0	−274
4. $\sigma_g^2\pi_u^4\sigma_g^2\delta_g^2\delta_u^{*2}\pi_g^{*3}\sigma_u^{*1}$ ($^7\pi_u$)	−6.18	137	−6.59	177	−6.46	229
5. $\sigma_g^2\pi_u^4\sigma_g^2\delta_g^2\delta_u^{*2}\pi_g^{*4}$ ($^5\Sigma_g$)	−4.92	170	−5.11	211	−4.91	256

[a] mhf: magnetic hyperfine field (only dipolar and Fermi contact interactions).

$(3d\sigma_u^*)^{1.49}(4s\sigma_g)^{2.0}$ configuration as the electronic ground state with an equilibrium internuclear distance of 2.4 Å. This distance is larger than the recently measured Fe–Fe distance using the EXAFS technique.[22] According to the HF–CI calculations the chemical bond between iron atoms is a single bond and it is almost entirely due to $4s\sigma_g$ molecular orbital.

Guenzburger and Saitovich[23] reported DVM–Xα calculations on Fe dimers, and they have calculated hyperfine parameters, specifically IS, QS, and magnetic hyperfine fields. Their idea is to search for the ground-state configuration by looking at the calculations that agreed at least in sign and magnitude with the experimental values of the hyperfine parameters. They have carried out all the calculations for the Fe–Fe distance of 1.87 Å.[22]

The Xα–SW function is a more complicated function of the Xα parameters such as sphere radii, exchange parameter α, size of the basis, etc.[17] In our calculations, the basis functions employed were s, p, d, and f waves on outer sphere as well as on transition metal atoms. The inclusion of "g" functions did not alter the wave functions and thus it was omitted. The α-parameter for Fe and Cr are the Schwarz values[24] which satisfy the virial theorem for isolated atoms. The α value for the intersphere region and the outer sphere is the valence electron weighted average of the atoms. The Norman criterion[16] was used to find the atomic sphere radii. The outer sphere was always considered tangential to Norman spheres.

The one-electron properties calculated for Xα-SW functions were found to be dependent on the degree of overlap between Norman spheres. The spin-polarized calculations were performed for all the probable configurations with an Fe–Fe distance of 2 Å for overlaps of 0%, 25%, and 30%. Although Xα statistical total energies are not very accurate, the relative values for various configurations can be compared for a given overlap in order to find the lowest energy configuration. For all the overlaps, $^7\Delta_u$ with $(\sigma_g^2\pi_u^4\sigma_g^2\delta_g^3\delta_u^{*2}\pi_g^{*2}\sigma_u^{*1})$ configuration shows the lowest energy, similar to the density functional method.[20]

Hyperfine parameters were obtained from the calculated molecular wave function in a way very similar to the method adopted by Guenzburger et al.[23] The isomer shift (IS) is proportional to $\Delta\rho(0)$ where $\rho(0)$ is the electronic charge density at the nucleus given by

$$\rho(0) = \sum_i n_i|\Psi_i(0)|^2$$

Ψ_i is a molecular orbital with occupation n_i. The quadrupole interaction Δ is due to the interaction between the nonspherical charge distribution of the nucleus and the electric field gradient (EFG) caused by the electrons or other ions in the crystal. All the electrons are considered in the calculations; hence

$$\Delta = \Delta_e + \Delta_n = \tfrac{1}{2}e^2Q\left[q + Z\frac{(3z^2 - r^2)}{r^5}\right]$$

where

$$q = -\sum_i n_i\left\langle\Psi_i(\vec{r})\left[\frac{3\cos^2\theta - 1}{r}\right]\Psi_i(\vec{r})\right\rangle$$

Δ_e = electronic contribution, and Δ_n is the nuclear contribution; Z is the atomic number of the other atom. It should be noted that in the Xα–SW method the inner cores are spherically averaged and hence need the Sternheimer core polarization corrections.[25]

The magnetic hyperfine interaction originates from the interaction between the magnetic hyperfine field produced by the electrons and the nuclear spin. There are three types of contribution: orbital, spin dipolar, and contact. In ref 23 the orbital contribution is neglected with the hope that orbital momentum may be quenched to a certain extent. The neglect of the orbital contribution might be a serious error particularly for states other than Σ states. Even for such cases there will be a mixing of other states due to configuration interactions (multiplet structure) which are neglected in the calculations. It should also be mentioned that the Xα exchange approximation underestimates the spin polarization of the core electrons.[23] It is our opinion that magnetic hyperfine fields (mhf) as calculated from the Xα method are not very reliable and hence one has to be cautious in deciding the electronic ground state based on the calculated magnetic hyperfine field at the nucleus. We also noticed that the contact contribution was very sensitive to the degree of overlap compared to other one-electron properties. We have thus used mainly the quadrupole interaction for comparison with the experimental results.

With Xα approximations, in contrast to the ab initio HF–CI calculations, all configurations indicated a bonding due to d orbitals in addition to s orbits. Table II lists the low-lying configurations which give QS values matching in sign and closer in magnitude to the experimental value. The bond order lies between 1.7 and 2.9 for the above configurations. $^7\Sigma_g$ has the lowest bond order. For configurations 1, 2, and 4 there is bonding due to d and s electrons and π bonding due to d electrons; configuration 3 gives σ bonding mainly due to s electrons and π bonding due to d electrons; configuration 5 shows only σ bonding (s and d electrons). According to Moskovits et al.,[6] the experimental values of the M–M stretching force constant (k) for Fe_2 and Cu_2 are not far away from the single-bond value calculated from Sieberts' method.

(22) P. A. Montano and G. K. Shenoy, *Solid State* Commun., **35**, 53 (1980); H. Purdum, P. A. Montano, G. K. Shenoy, and T. Morrison, *Phys. Rev. B*, **1**, (1982).
(23) D. Guenzburger and E. M. B. Saitovitch, *Phys. Rev.*, **24**, 2368 (1981).
(24) K. Schwarz, *Phys. Rev. B*, **5**, 2466 (1972).
(25) R. M. Sternheimer, *Phys. Rev.*, **130**, 1423 (1963); R. P. Gupta and S. K. Sen, *Phys. Rev. A*, **8** 1169 (1973).

Table III. Hyperfine Parameters for Fe_2 at Equilibrium Distances (30% Overlap)

config	equilib distance, Å	$X\alpha$ statist total energy, au	QS mm/s without Sternheimer correction	QS mm/s Sternheimer factor, $R = 0.32$	QS mm/s with $R = 0.2$, $Q = 0.16$ b	mhf, kOe	$\rho(0)$, au
1. $(^7\Delta_u)$	2.0	−5045.400	−2.78	−1.89	−1.69	109	11 071.163
2. $(^9\Sigma_g)$	2.2	−5045.372	−6.34	−4.31	−3.86	900	11 073.331
3. $(^7\Sigma_g)$	2.1	−5045.361	−6.88	−4.67	−4.19	−340	11 072.210
4. $(^7\pi_u)$	2.2	−5045.327	−6.38	−4.34	−3.88	118	11 071.049
5. $(^5\Sigma_g)$	2.3	−5045.14	−5.0	−3.40	−3.04	208	11 070.811

For molecules such as V_2, Ti_2, and Ni_2, the experimental values of k are much higher than the single-bond values. This could be due to the presence of multiple bonds due to d electrons in the later molecules. Although in the case of Fe_2, the experimental value of k (1.48) is only slightly larger than the single-bond value (1.19), the difference between the two values is larger than that of the Cu_2 molecule where the bond order is essentially single.[6] The above consideration could mean bonding due to d electrons in the case of Fe_2. This is in agreement with our analysis of the $X\alpha$–SW calculations. Because of the lower bond order, $^7\Sigma_g$ seems to be the most probable ground state, consistent with all the experimental results.

The calculated QS without Sternheimer correction for various configurations of Fe_2 at an Fe–Fe distance of 2 Å are listed (Table II) with different degrees of overlap along with the magnetic hyperfine fields (spin dipolar and Fermi contact only). The quadrupole moment of ^{57}Fe nucleus is taken to be 0.21 b.[26] For all overlaps $^7\Delta_u$ gives the right sign for the QS but the magnitude is too small compared to the experimental value (−4.08 mm/s) which is measured with great accuracy. The HF–CI calculations also give a smaller value for the QS for $^7\Delta_u$, the contribution to the EFG being $-^4/_7(0.51)\langle 1/r^3\rangle$. The reason for the discrepancy between the experimental and calculated values in the case of HF–CI calculations could be due to the neglect of the spin–orbit interaction which would mix the different states. In fact, the $^7\Sigma_g$ state is only about 0.002 eV above the $^7\Delta_u$ state with almost similar electronic configuration. The spin–orbit interaction is larger compared to the very small difference in energies between the various states. Of course, in the present $X\alpha$ calculations we have neglected configuration interactions in addition to the spin–orbit interaction. It is hoped that, although one-electron approximation is used, the Coulomb correlation effects are taken into account at least partially through $X\alpha$ exchange.[23,27] The $X\alpha$ calculations also show a contribution to EFG from 4p electrons: $\langle 1/r^3\rangle_{4p}$ is almost 2 to 3 times larger than $\langle 1/r^3\rangle_{3d}$. Hence, the electric field gradients are influenced by the population of 4p states.

We also calculated the $X\alpha$ statistical total energy as a function of the internuclear distance. The equilibrium distance and the $X\alpha$ statistical total energy at the equilibrium distance along with the QS and the magnetic hyperfine fields are listed in Table III. Although $^7\Delta_u$ is the lowest energy state, it gives a smaller quadrupole splitting even without the Sternheimer correction factor.[25] The Sternheimer correction is given by $(1 - R)$, with R around 0.2.[28] A positive R factor reduces the EFG at the nucleus. Hence, $^7\Delta_u$ has a further reduction in QS, making the discrepancy even larger. Other than $^7\Delta_u$, the configurations giving $^9\Sigma_g$ are lower in energy than all others. The QS without Sternheimer factor are larger compared to the experimental value but with a Sternheimer factor of 0.32,[26] the calculated QS values are closer to the experimental value. The QS with the Sternheimer factor of $R = 0.32$ are listed in Table III.

The observed QS of −4.08 ± 0.06 mm/s for Fe_2 is the largest among all the iron compounds.[28] In most of the iron compounds, the observed QS could be accounted as almost due to 1 d electron in one of the d orbitals.[28] The contributions to the EFG due to various d electrons are listed in Table IV along with the QS (without Sternheimer correction) calculated with $Q = 0.21$ b and atomic $\langle 1/r^3\rangle_{3d} = 5$ au.[29] The QS due to 1 d_z electron is −6.06 mm/s, which is large compared to any experimentally measured QS of any Fe compound. The QS is influenced by several factors such as (1) magnitude of Q, (2) Sternheimer shielding and antishielding factors, (3) contributions from p electrons, (4) covalency effects, etc. The $\langle 1/r^3\rangle_{3d}$ values calculated from the present calculations are fairly accurate (average $\langle 1/r^3\rangle_{3d}$ for bonding orbitals ≈4 au and for antibonding orbitals ≈6 au, giving an average of 5 au closer to atomic Fe).[29] Several authors have pointed out that the value of the Sternheimer correction $R = 0.32$ is incorrect and a value of R between 0.05 and 0.2 is more reliable.[30–32] With a smaller value of R, the agreement between the experimental and calculated values needs a reduction in the Q value. With $R = 0.2$, Q has to be reduced by 20 to 25%. This is in agreement with a smaller value of Q calculated in ref 31. The DVM–$X\alpha$ calculations give QS values ($^7\Sigma_g$ and $^9\Sigma_g$) much larger than the experimental value. Again these results indicate a requirement of reduction in Q value by 20 to 30% in agreement with the above analyses. In Table V a comparison is given between the different theoretical calculations and the experimental measurements of the QS in Fe_2.

Table IV. EFG and QS Calculated with $Q = 0.21$ b and $\langle 1/r^3\rangle_{3d} = 5$ au[29] for One Electron in a d Orbital without Sternheimer Correction

orbital	EFG	QS, mm/s
$d_{z^2-r^2}$	$-^4/_7e\langle 1/r^3\rangle$	−6.06
d_{xz}	$-^2/_7e\langle 1/r^3\rangle$	−3.03
d_{yz}	$-^2/_7e\langle 1/r^3\rangle$	−3.03
$d_{x^2-y^2}$	$^4/_7e\langle 1/r^3\rangle$	6.06
d_{xy}	$^4/_7e\langle 1/r^3\rangle$	6.06

As mentioned earlier, mhf are not calculated accurately in the $X\alpha$ approximations. The discrepancy between the experimental value (660 kOe) and the calculated values (900 kOe for $^9\Sigma_g$ and −340 kOe for $^7\Sigma_g$) could be due to the underestimation of spin polarization of the core electrons.[23,27] Hence, according to $X\alpha$–SW calculations, $^9\Sigma_g$ or $^7\Sigma_g$ seems to be the most probable ground state of the Fe_2 molecule. The $X\alpha$–SW calculations overestimate the equilibrium distances by about 0.15 Å[33,18a] for diatomic molecules and hence, for the above configurations, the equilibrium distances are reasonably in agreement with the experimental value.[22] It is noted that the calculated ground-state symmetry is in good agreement with the one predicted in ref 9. In ref 7–9 symmetry considerations were used to predict the ground state. The analysis was carried out under the assumption that only one d electron contributes to the EFG. Although this may seem an oversimplification of the problem, the reality is that all Fe–3d atom

(26) R. Ingalls, *Phys. Rev.*, **128**, 1155 (1962).
(27) J. C. Slater, "Quantum Theory of Molecules and Solids", Vol. IV, McGraw-Hill, New York, 1974.
(28) N. N. Greenwood and T. C. Gibb, "Mössbauer Spectroscopy", Chapman and Hall, London, 1971.
(29) P. S. Bagus and B. Liu, *Phys. Rev.*, **148**, 79 (1966).
(30) R. M. Sternheimer, *Phys. Rev.*, **A6**, 1702 (1972).
(31) K. J. Duff, K. C. Mishra, and T. P. Das, *Phys. Rev. Lett.*, **46**, 1611 (1981); S. Vajda, G. D. Sprouse, M. H. Fatailovich, J. W. Noe, *Phys. Rev. Lett.*, **47**, 1230 (1981).
(32) S. N. Ray and T. P. Das, *Phys. Rev. B*, **16**, 4794 (1977).
(33) D. R. Salahub, R. P. Messmer, and K. H. Johnson, *Mol. Phys.*, **31**, 529 (1976).
(34) S.-S. Lin and A. Kant, *J. Phys. Chem.*, **73**, 2450 (1969).

Table V. Theoretical Calculations of Ground State and QS for Fe_2

method	equilib distance, Å	electronic ground state	configuration	QS (mm IS)	ref
density functional method	2.1	$^7\Delta_u$	$\sigma_g^2\pi_u^4\sigma_g^2\delta_g^3\delta_u^{*2}\pi_g^{*2}\sigma_u^{*1}$	-3.03^a -1.84^b	20
HF-CI	2.4	$^7\Delta_u$	$\sigma_g^{1.57}\pi_u^{3.06}\delta_g^{2.53}\delta_u^{*2.47}\pi_g^{*2.87}\sigma_u^{*1.49}\sigma_g^{2.0}$	-3.12^a -1.90^b	21
DVM-Xα	1.87	$^7\Pi_u$	$\sigma_g^2\pi_u^4\sigma_g^2\delta_g^2\delta_u^{*2}\sigma_u^{*1}\pi_g^{*3}$	−4.6	23
experimental	1.87			−4.08 ± 0.06	
SCF-Xα-SW	*c*				*d*

[a] QS calculated with $Q = 0.21$ b and $\langle 1/r^3\rangle_{3d} = 5$ au and without Sternheimer correction factor. [b] QS calculated with $Q = 0.16$ b and $R = 0.2$. [c] See Table III. [d] This work.

Table VI. Hyperfine Parameters for FeCr at $R = 2.0$ Å (30% Overlap, Restricted Calculation)

config	X statist total energy, au	QS, mm/s, without Sternheimer correction	QS, mm/s, with Sternheimer factor 0.2 and $Q = 0.16$ b
1. $\sigma^2\sigma^2\pi^4\delta^3\delta^{*3}$ ($^3\Gamma$)	−4607.15	2.84	1.74
2. $\sigma^2\sigma^2\pi^4\delta^2\delta^{*2}\pi^{*2}$ ($^7\Sigma$)	−4607.00	−4.87	−2.97
3. $\sigma^2\sigma^2\pi^3\delta^3\delta^{*2}\pi^{*2}$ ($^7\phi$)	−4606.90	2.47	1.51
4. $\sigma^2\sigma^2\pi^3\delta^2\delta^{*2}\pi^{*3}$ ($^7\Delta$)	−4606.74	−4.48	−2.73

diatomics as well as the majority of Fe^{2+} compounds show properties that can be described using single-electron approximations.

For FeCr molecules, we do not have any information about the magnetic hyperfine field at the ^{57}Fe nucleus. Hence, only restricted Xα–SW calculations were performed on FeCr with a Fe–Cr distance of 2.0 Å. This distance is closer to the average of the covalent distances of Fe_2 (2.0 Å) and Cr_2 (1.9 Å).[11] The sign of V_{zz} is also not known for FeCr. The low-energy configurations which give the magnitude of the QS closer to the experimental QS (2.9 mm/s) are listed in Table VI. A Sternheimer factor of $R = 0.2$ and $Q = 0.16$ b was used. The same value of R was used because the bonding between Fe and Cr atoms is predominantly unpolarized and almost completely covalent. The configurations of Fe in Fe_2 and FeCr have almost the same number of d electrons (≃6.5). The configuration 1. ($^3\Gamma$) gives the right magnitude (2.84 mm/s) without the Sternheimer correction factor and with $Q = 0.21$ b. If such is the case, the coupling between Fe and Cr would be antiferromagnetic. The configuration 2. ($^7\Sigma$) gives the right magnitude with $R = 0.2$ and $Q = 0.16$ b, indicating a ferromagnetic coupling between Fe and Cr atoms. The bond between Fe and Cr atoms is due to both d and s electrons. The configuration 4. ($^7\Delta$) also gives a QS very close to the one observed experimentally.

Conclusions

1. Various iron–chromium clusters were isolated in rare gas matrices and identified by Mössbauer spectroscopy. An IS = 0.12 mm/s for FeCr molecules indicates a decrease in the s electron density at the Fe nucleus. The trend of IS for various iron–chromium clusters indicated that the small (FeCr) clusters may not be representative of bulk.

2. Xα–SW calculations were performed on Fe_2 and FeCr molecules, and an attempt is made to explain the nature of bonding between the two atoms. Calculations must be consistent with experimental measurements such as interatomic distances, QS, IS, and magnetic hyperfine splitting. (The last two parameters cannot be fitted without taking full configuration interaction as well as spin–orbit coupling into consideration.) The most probable ground state for Fe_2 is a $^7\Sigma_g$ (lowest bond order consistent with low dissociation energy ≈1 eV) and for FeCr, either $^7\Sigma$ or $^7\Delta$. The calculations indicated a need for a lower value for the quadrupole moment of the ^{57}Fe nucleus in agreement with ref 31.

Acknowledgment. The authors wish to thank Dr. Michel Cook of Harvard University for providing Xα–SW programs and for helpful discussions. We also thank Drs. Irene Shim and Karl A. Gingerich for providing the ab initio HF–CI results on Fe_2 molecules prior to publication.

Registry No. Fe_2, 12596-01-9; FeCr, 12052-89-0.